Geoscience Frontiers (2010) 1, 91–97

available at www.sciencedirect.com

China University of Geosciences (Beijing)

Geoscience Frontiers

journal homepage: www.elsevier.com/locate/gsf

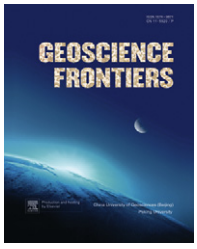

ORIGINAL ARTICLE

Thermal expansion of kyanite at ambient pressure: An X-ray powder diffraction study up to 1000 °C

Xi Liu [a,b,*], Qiang He [a,b], Hejing Wang [a,b], Michael E. Fleet [c], Xiaomin Hu [a,b]

[a] *The Key Laboratory of Orogenic Belts and Crustal Evolution, Ministry of Education of China, Beijing 100871, China*
[b] *School of Earth and Space Sciences, Peking University, Beijing 100871, China*
[c] *Department of Earth Sciences, University of Western Ontario, London, Ontario, N6A 5B7, Canada*

Received 22 June 2010; accepted 12 July 2010
Available online 23 September 2010

KEYWORDS
High temperature;
Kyanite;
Thermal expansion;
X-ray powder diffraction

Abstract The thermal expansion coefficients of kyanite at ambient pressure have been investigated by an X-ray powder diffraction technique with temperatures up to 1000 °C. No phase transition was observed in the experimental temperature range. Data for the unit-cell parameters and temperatures were fitted empirically resulting in the following thermal expansion coefficients: $\alpha_a = 5.8(3) \times 10^{-5}$, $\alpha_b = 5.8(1) \times 10^{-5}$, $\alpha_c = 5.2(1) \times 10^{-5}$, and $\alpha_V = 7.4(1) \times 10^{-3}$ °C^{-1}, in good agreement with a recent neutron powder diffraction study. On the other hand, the variation of the unit-cell angles α, β and γ of kyanite with increase in temperature is very complicated, and the agreement among all studies is poor. The thermal expansion data at ambient pressure reported here and the compression data at ambient temperature from the literature suggest that, for the kyanite lattice, the most and least thermally expandable directions correspond to the most and least compressible directions, respectively.

1. Introduction

Kyanite, andalusite and sillimanite are polymorphs with a composition of Al_2SiO_5. Their relative stability has been extensively investigated because of their importance in metamorphic petrology (Kerrick, 1990, and references therein). However, their exact phase relationships remain controversial because of the very slow polymorphic phase transitions resulting from small differences in their structures and thermodynamic properties (Robie et al., 1995, and references therein). It is generally understood that kyanite has the largest P–T stability field; according to the high-P experimental data, kyanite breaks down to stishovite and corundum at about 16 GPa (Liu, 1974; Irifune et al., 1995; Schmidt et al., 1997; Liu et al., 2006; Ono et al., 2007). Kyanite is also a very important high-P phase for

* Corresponding author. The Key Laboratory of Orogenic Belts and Crustal Evolution, Ministry of Education of China, Beijing 100871, China. Tel.: +86 10 6275 3585; fax: +86 10 6275 2996.
E-mail address: xi.liu@pku.edu.cn (X. Liu).

Peer-review under responsibility of China University of Geosciences (Beijing).
doi:10.1016/j.gsf.2010.07.002

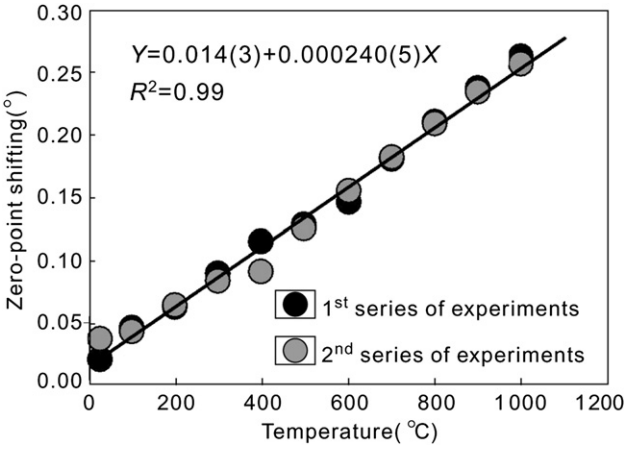

Figure 1 Zero-point shift vs. temperature. Solid circles are for the 1st series of experiments; shaded circles are for the 2nd series. The line and equation are based on all data. See text for the details of the calculation.

materials of the continental crust and deeply buried pelagic sediments, so that knowledge of its physical properties is of importance to understanding geodynamic processes in the mantle (Irifune et al., 1994; Schmidt et al., 2004; Rapp et al., 2008). Additionally, kyanite plays a significant role in a large number of geological reactions, particularly those involving mineral phases such as paragonite, zoisite, lawsonite, pumpellyite, chloritoid, staurolite, stishovite, etc. (e.g. Chatterjee, 1972; Liu, 1974; Schreyer, 1988; Irifune et al., 1995; Poli and Schmidt, 1995; Schmidt et al., 1997; Liu et al., 2006; Ono et al., 2007). In order to fully understand these reactions and their phase relations it is necessary to accurately constrain the thermodynamic properties of kyanite, including compressibility and thermal expansion.

The compressibility of kyanite under high pressures has been investigated both by high-pressure experiments (Brace et al., 1969; Comodi et al., 1997; Yang et al., 1997a; Friedrich et al., 2004; Liu et al., 2009) and by theoretical simulations (Matsui, 1996; Oganov and Brodholt, 2000; Winkler et al., 2001). As summarized by Liu et al. (2009), the bulk modulus and its pressure derivative of kyanite at ambient temperature have been well established, and are close to 196 ± 6 GPa and 4, respectively.

In contrast, the thermal expansion of kyanite at high temperatures has been investigated in only three experimental studies (Skinner et al., 1961; Winter and Ghose, 1979; Gatta et al., 2006). Skinner et al. (1961) collected X-ray diffraction data on a kyanite powder that was heated up to 1055 °C, but they calculated the unit-cell parameters by using only six *d*-spacings. Unfortunately, kyanite has low symmetry (space group $P\bar{1}$), and the determination of six unknowns (a, b, c, α, β and γ) from six independent equations is questionable. Winter and Ghose (1979) collected single-crystal X-ray data at 25, 400, 600 and 800 °C, from which they determined the unit-cell dimensions of kyanite. Their limited data, however, showed apparent deviation from the trends defined by Skinner et al. (1961), especially at high temperatures. Recently, Gatta et al. (2006) carried out a neutron powder diffraction study at ambient temperature and in the temperature range of 600−1200 °C. Putting aside the large gap between room temperature and 600 °C, the thermal expansion coefficients obtained in this study are generally in good agreement with those of Winter and Ghose (1979) but the changes

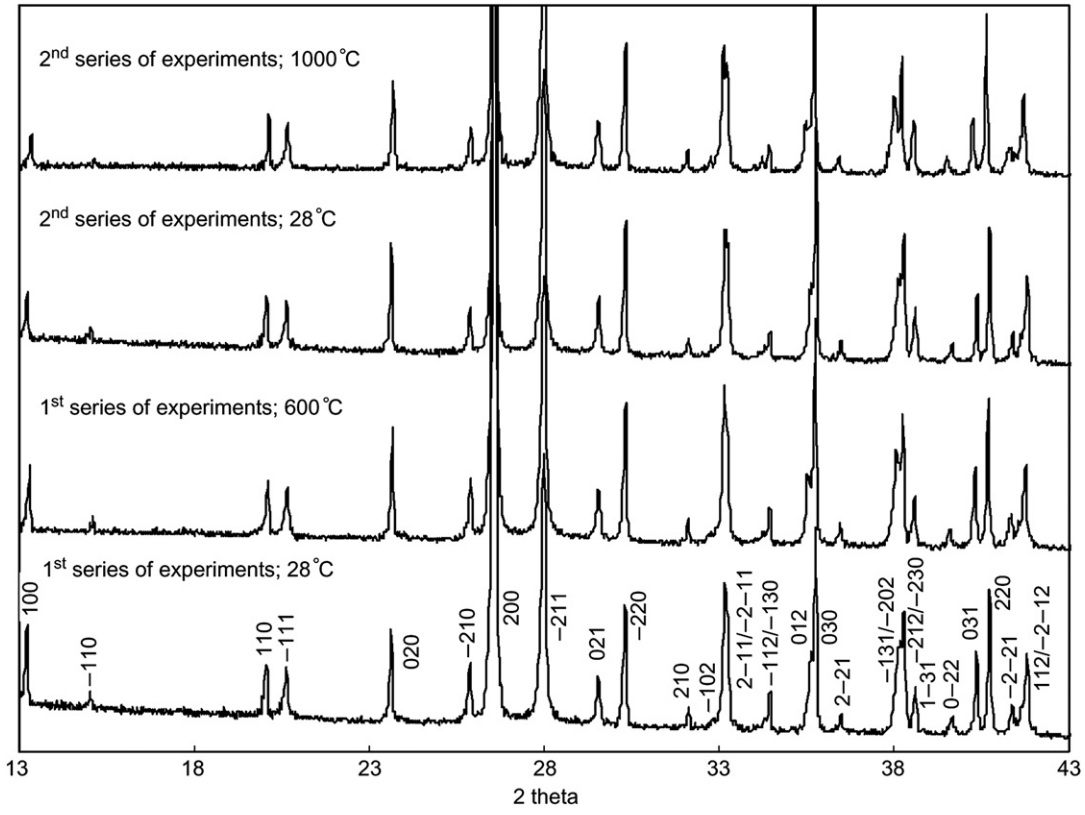

Figure 2 Examples of the X-ray diffraction patterns of kyanite at ambient temperature, 600 °C and 1000 °C (without correcting the zero-point shift).

Table 1 Unite-cell parameters of kyanite vs. temperature.

T(°C)	a(Å)	b(Å)	c(Å)	α(°)	β(°)	γ(°)	V(Å^3)
1st series of experiments							
28	7.1166(10)	7.8466(7)	5.5737(7)	89.99(1)	101.10(1)	105.99(1)	293.14(4)
100	7.1180(9)	7.8490(6)	5.5760(6)	90.00(1)	101.08(1)	105.98(1)	293.44(4)
200	7.1220(12)	7.8540(9)	5.5793(8)	90.01(1)	101.08(1)	105.96(1)	293.99(5)
300	7.1289(15)	7.8594(11)	5.5847(10)	90.04(2)	101.05(2)	105.96(1)	294.81(7)
400	7.1363(12)	7.8680(9)	5.5916(9)	90.01(1)	101.07(2)	105.97(1)	295.76(5)
500	7.1460(13)	7.8717(10)	5.5949(9)	90.01(1)	101.07(2)	105.97(1)	296.25(6)
600	7.1443(14)	7.8755(10)	5.6000(10)	90.00(1)	101.07(2)	105.97(1)	296.83(6)
700	7.1504(15)	7.8836(10)	5.6077(9)	90.02(1)	101.02(2)	105.96(1)	297.86(6)
800	7.1561(16)	7.8902(11)	5.6137(10)	90.00(2)	101.05(2)	105.95(1)	298.66(6)
900	7.1682(10)	7.8960(6)	5.6183(7)	89.91(1)	101.06(1)	106.01(1)	299.55(4)
1000	7.1763(15)	7.9058(10)	5.6225(11)	89.85(2)	101.11(2)	106.05(2)	300.39(6)
2nd series of experiments							
28	7.1203(9)	7.8484(6)	5.5758(6)	90.00(1)	101.09(1)	106.00(1)	293.47(4)
100	7.1217(10)	7.8497(8)	5.5766(6)	90.02(1)	101.08(1)	105.99(1)	293.64(4)
200	7.1259(14)	7.8558(9)	5.5823(9)	90.01(1)	101.05(2)	105.98(1)	294.39(6)
300	7.1309(14)	7.8608(10)	5.5854(10)	90.02(1)	101.05(2)	105.97(1)	294.96(6)
400	7.1315(21)	7.8644(13)	5.5883(12)	90.03(2)	101.03(2)	105.95(2)	295.33(8)
500	7.1347(27)	7.8722(17)	5.5917(17)	90.07(2)	100.96(3)	105.92(2)	296.04(10)
600	7.1404(22)	7.8823(16)	5.5980(13)	90.08(2)	100.98(2)	105.90(2)	297.00(9)
700	7.1525(16)	7.8866(10)	5.6101(9)	90.02(1)	101.04(2)	105.96(1)	298.16(6)
800	7.1625(9)	7.8919(5)	5.6124(9)	89.92(1)	101.10(1)	105.99(1)	298.81(5)
900	7.1666(14)	7.8957(9)	5.6181(11)	89.96(2)	101.05(2)	105.98(1)	299.50(6)
1000	7.1746(11)	7.9009(8)	5.6233(8)	89.93(2)	101.07(1)	106.00(1)	300.27(5)

with temperature of the unit-cell angles of kyanite are not. Clearly, further investigation on the thermal expansion of kyanite is necessary.

This study was designed to evaluate the thermal expansion of kyanite at ambient pressure using an X-ray powder diffraction technique.

2. Experimental details

The natural kyanite used in this study was taken from Liu et al. (2009). X-ray fluorescence spectrometry at the Department of Earth Sciences, University of Western Ontario indicated a chemical formula of $(Al_{1.99}Fe_{0.01})SiO_5$ for this material (Liu et al., 2009). The material was also characterized using the powder X-ray diffractometer hosted at the School of Earth and Space Sciences, Peking University (X'Pert Pro MPD system; Cu Kα1 X-ray radiation): kyanite was confirmed to be the only solid crystalline phase, with the room-temperature unit-cell parameters of $a = 7.115(2)$ Å, $b = 7.841(2)$ Å, $c = 5.573(2)$ Å, $\alpha = 90.01°(3)$, $\beta = 101.13°(3)$ and $\gamma = 105.96°(3)$, which are essentially identical to the values from the JCPDS reference pattern card 11−46. Its unit-cell volume at ambient pressure was determined to be 292.8 ± 0.1 Å^3.

High-temperature X-ray diffraction experiments on kyanite at ambient pressure were carried out as well with the X'Pert Pro MPD system at the School of Earth and Space Sciences, Peking University. An attached Anton Paar HTK − 1200N oven with a Eurotherm temperature controller (Eurotherm 2604; type S thermocouple) was used to heat up the sample (about 0.20−0.25 g in mass). The maximum temperature achievable with this heating system is 1200 °C with an accuracy of ±2 °C; the controlling thermocouple was checked against the melting point of NaCl. The oven ran in a vacuum chamber with a nickel window, in order to protect the heating element. The X'Pert Pro MPD diffractometer system was equipped with a Cu target, and was operated at 40 kV, 40 mA, with a scanning step length in our experiments of 0.017°2θ. The alignment was done at ambient temperature only with a standard of silicon crystalline powder.

Two series of experiments were conducted up to 1000 °C, with the material from the first series reused in the second. The heating and data-collection procedures were as follows: after collection of X-ray diffraction data at a given temperature, the sample was heated up to the next setpoint using a fixed ramp; the kyanite

Table 2 Thermal expansion coefficients of kyanite.

Data source	a	b	c	v
This study	$5.8(3) \times 10^{-5}$	$5.8(1) \times 10^{-5}$	$5.2(1) \times 10^{-5}$	$7.4(2) \times 10^{-3}$
Skinner et al. (1961)	$6.9(2) \times 10^{-5}$	$6.6(1) \times 10^{-5}$	$6.0(2) \times 10^{-5}$	$8.3(2) \times 10^{-3}$
Winter and Ghose (1979)	$5.6(5) \times 10^{-5}$	$5.1(1) \times 10^{-5}$	$6.0(3) \times 10^{-5}$	$7.4(2) \times 10^{-3}$
Gatta et al. (2006)	$5.3(1) \times 10^{-5}$	$5.8(1) \times 10^{-5}$	$5.2(1) \times 10^{-5}$	$7.4(1) \times 10^{-3}$

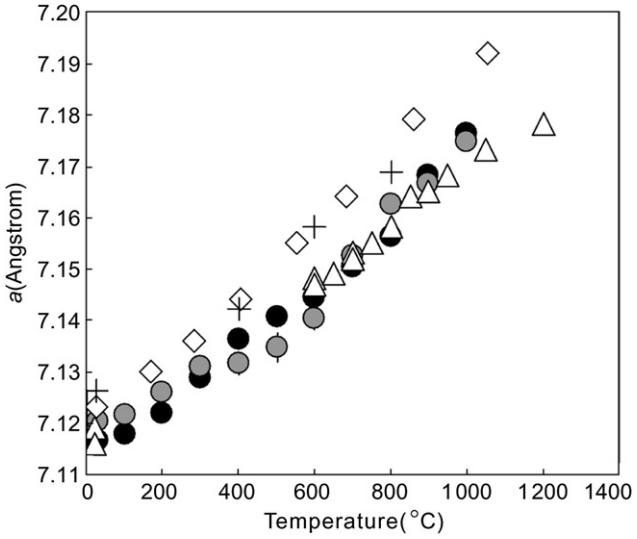

Figure 3 Variation of *a*-axis of kyanite with temperature. Solid circles, data collected at different temperatures in the 1st series of experiments; shaded circles, data collected at different temperatures in the 2nd series of experiments; empty triangles, data from Gatta et al. (2006); pluses, data from Winter and Ghose (1979); diamonds, data from Skinner et al. (1961). For most data, error bars are smaller than or equal to symbol size.

sample was then allowed to relax before collection of the powder diffraction spectrum. In the first series of experiments, the heating ramp was 10 °C/min, the equilibration time was 5 min and data were collected between 10 and 80°2θ. The same parameters in the second experimental series were 2°C/min, 10 min, and 10−120°2θ, respectively. The thermal relaxation interval of the sample was, thus, evaluated by changing the heating ramp and the equilibration time: as detailed below, these two heating and data-collection procedures generated essentially identical results.

According to our experimental procedure, realignment of the experimental system was not made for high temperature. Because

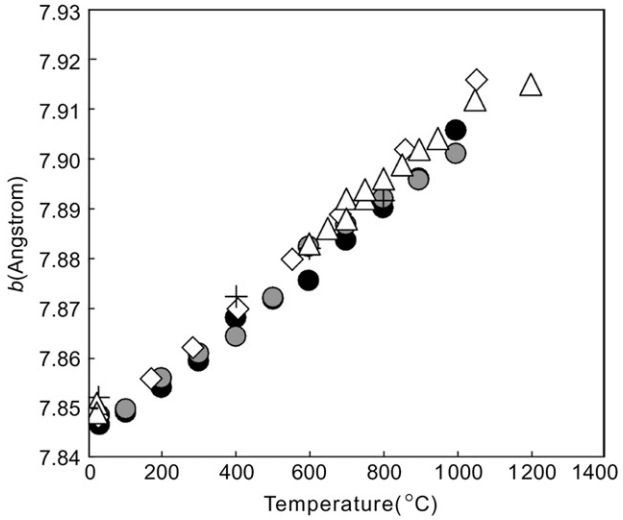

Figure 4 Variation of *b*-axis of kyanite with temperature. See the caption of Fig. 3 for the symbol information and datum sources. For most data, error bars are smaller than or equal to symbol size.

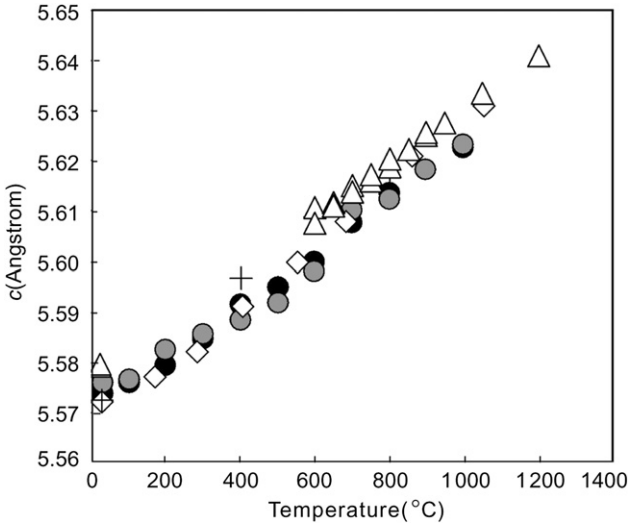

Figure 5 Variation of *c*-axis of kyanite with temperature. See the caption of Fig. 3 for the symbol information and datum sources. For most data, error bars are smaller than or equal to symbol size.

of the thermal expansion of the furnace and sample holder components, the sample position is slightly, but progressively elevated as temperature is increased, so that the X-ray diffraction data are subjected to a small zero-point shift. As a first-order approximation, we used the peak positions of the well-resolved reflection lines 100 and 200, obtained from the raw X-ray diffraction patterns, to calculate the zero-point shift:

$$\sin\left(\frac{\phi_2-\delta}{2}\right)=2\sin\left(\frac{\phi_1-\delta}{2}\right),$$

where ϕ_1, ϕ_2 and δ are the 2θ value of the peak 100, 2θ value of the peak 200, and zero-point shift, respectively. The results are shown in Fig. 1, and are well represented by the equation $\delta = 0.014(3) + 0.000240(5) \times T$ with δ in ° and T in °C. Testing was also done with different peak pairs such as 100 and 500, and no real difference was found. Subsequently, small adjustments according to our regressed equation were made to the raw X-ray diffraction patterns before we fully processed them to determine the unit-cell parameters.

Kyanite is of low symmetry (space group $P\bar{1}$) and has large unit-cell parameters. Consequently, in order to achieve good data quality, kyanite should be probed by X-ray radiation of long wavelength whenever possible. Both this study and that of Skinner et al. (1961) used copper as the X-ray target. As shown in Fig. 2, even with the Cu Kα1 X-ray radiation, some peak overlap is still inevitable; for instance, peak 2−11 slightly overlaps with peak −2−11, peak −112 with peak −130, peak 012 with peak 030, peak −131 with peak −202, peak −212 with peak −230, and peak 112 with peak −2−12. Since Winter and Ghose (1979) used Mo as the X-ray source, and the wavelength of the neutrons in Gatta et al. (2006) was 1.09600 Å, a more severe peak-overlap would be expected in these two studies. To avoid the peak-overlap problem, we used only well-deconvolved peaks between 10 and 43°2θ to refine the unit-cell parameters. These peaks were 100, −110, 110, −111, 020, −210, 200, −211, 021, −220, 210, −102, 2−11, −2−11, −112, −130, 012, 030, 2−21, −131, −202, −212, −230, 1−31, 0−22, 031, 220, −2−21 and −2−12.

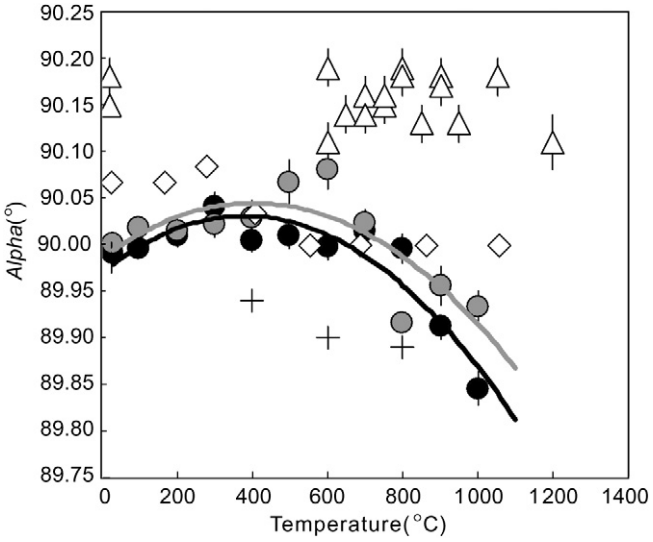

Figure 6 Variation of angle α of kyanite with temperature. See the caption of Fig. 3 for the symbol information and datum sources. Curves are fitted visually. For most data, error bars are smaller than or equal to symbol size.

3. Results and discussion

Both series of experiments were conducted up to 1000 °C at ambient pressure, and neither showed any apparent evidence of potential phase transition, in agreement with previous high temperature investigations (Skinner et al., 1961; Winter and Ghose, 1979; Gatta et al., 2006). According to published experimental data (Kerrick, 1990, and references therein), andalusite is the room-*P* stable form at high temperatures; prolonged heating of kyanite in this investigation did not produce any andalusite, evidencing the sluggish nature of the polymorphic phase transition. Typical X-ray powder diffraction patterns are shown in Fig. 2. The effect of temperature on the unit-cell parameters is summarized in Tables 1 and 2, and graphically illustrated in Figs. 3–9. For the purpose of comparison, the results of Skinner et al. (1961), Winter and Ghose (1979) and Gatta et al. (2006) are also plotted on those figures.

Figs. 3–5 show the variation of the unit-cell parameters *a*, *b* and *c* with temperature. In general, *a*, *b* and *c* increase almost linearly with increase in temperature. To keep the regression simple, the axial thermal expansion coefficients $(\alpha_j = l_j^{-1}(\partial l_j/\partial T))$ were eventually calculated by a linear regression through all the data points obtained in our experiments; they are $\alpha_a = 5.8(3) \times 10^{-5}$, $\alpha_b = 5.8(1) \times 10^{-5}$ and $\alpha_c = 5.2(1) \times 10^{-5}$ °C^{-1}. Comparing these values with the results in the literature (Table 2), we can find an excellent agreement among this X-ray powder diffraction study, the single-crystal X-ray diffraction study (Winter and Ghose, 1979) and the neutron powder diffraction study (Gatta et al., 2006). The earliest X-ray powder diffraction study done by Skinner et al. (1961) apparently resulted in larger thermal expansion coefficients, especially for the *a*-axis.

Figs. 6–8 show the variation of the unit-cell angles α, β and γ of the kyanite lattice with temperature increase. For all three angles, our data define complicated variation patterns: the α-angle appears to increase with temperature increase up to about 500 °C and then to decrease; the angles of β and γ, however, show the opposite trend. Additionally, the results show that large discrepancies clearly exist among all the experimental investigations. The values of the α-angle obtained by the neutron powder diffraction method (Gatta et al., 2006) are clearly larger than those constrained by the X-ray diffraction method (Fig. 6); and, Skinner et al.'s (1961) data clearly fall outside the main population of data points (see Figs. 7 and 8). This complicated situation most likely resulted from the fact that kyanite has low symmetry ($P\bar{1}$) and large unit-cell parameters. Therefore, high-temperature single-crystal X-ray diffraction would be desirable to resolve these discrepancies.

The volume–temperature data are shown in Fig. 9. Our data suggest that the unit-cell volume at 1000 °C is just ~2.4% larger than that at 28 °C, indicating a small volumetric thermal expansion coefficient for kyanite. We used the equation to linearly fit all

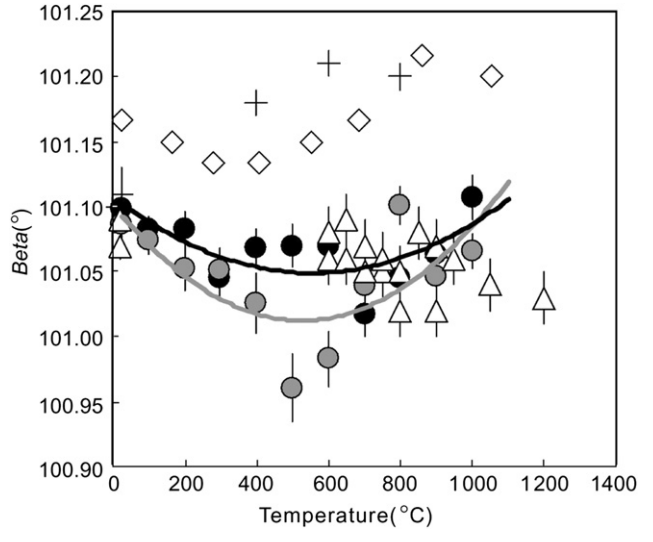

Figure 7 Variation of angle β of kyanite with temperature. See the caption of Fig. 3 for the symbol information and datum sources. Curves are fitted visually. For most data, error bars are smaller than or equal to symbol size.

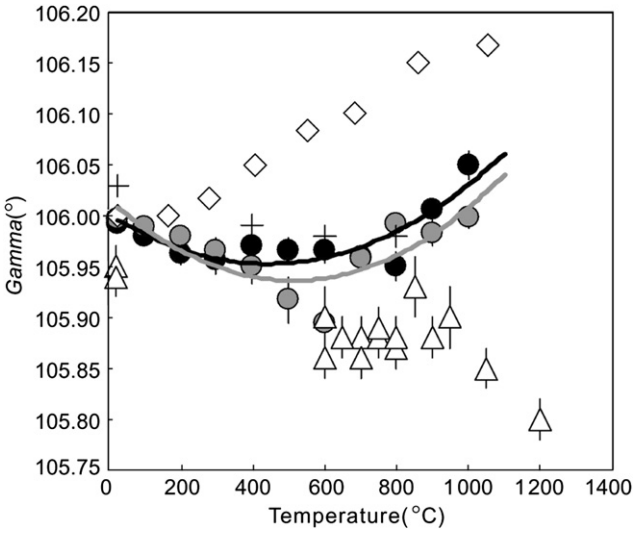

Figure 8 Variation of angle γ of kyanite with temperature. See the caption of Fig. 3 for the symbol information and datum sources. Curves are fitted visually. For most data, error bars are smaller than or equal to symbol size.

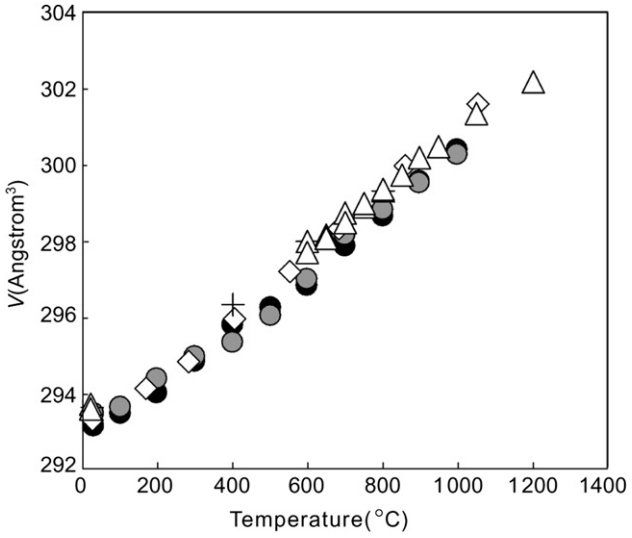

Figure 9 Variation of V of kyanite with temperature. See the caption of Fig. 3 for the symbol information and datum sources. For most data, error bars are smaller than or equal to symbol size.

our volume−temperature data, and obtained $\alpha_V = 7.4(1) \times 10^{-3}\ ^\circ C^{-1}$, which agrees perfectly with the results from Winter and Ghose (1979) and Gatta et al. (2006). In comparison, the volumetric thermal expansion coefficient determined by Skinner et al. (1961) now appears too large (Table 2).

For many silicate minerals, isobaric thermal expansion and isothermal compression have generally opposite effects on changes in crystal structure (Hazen and Finger, 1982; Yang et al., 1997b). As illustrated in Fig. 10, kyanite shows this behaviour: the c-axis has the largest compressibility and thermal expansibility, and the a-axis has the smallest compressibility and thermal expansibility. However, since kyanite is triclinic, it should be kept in mind that the principle axes of the strain ellipsoid do not coincide with the unit-cell axes.

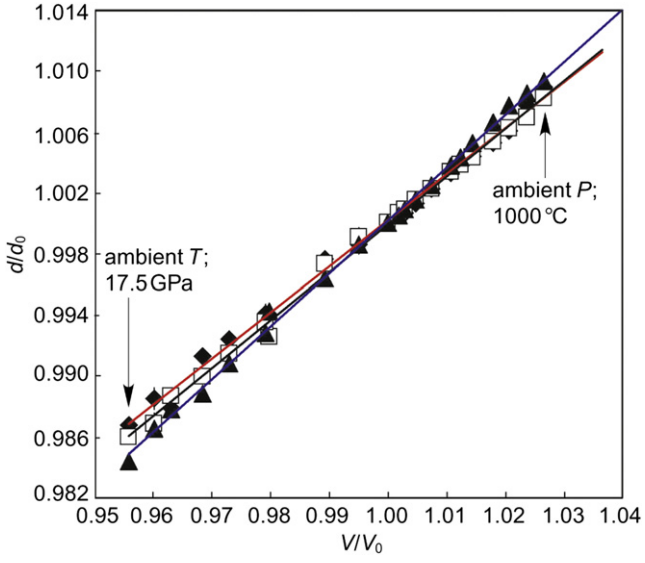

Figure 10 Variations of unit-cell dimensions (d/d_0) with V/V_0. Solid diamonds, axis a; empty squares, axis b; solid triangles, axis c. High-pressure data are from Liu et al. (2009).

For the three Al_2SiO_5 polymorphs, the volumetric thermal expansion coefficients generally increase in the sequence of andalusite > kyanite > sillimanite. The unit-cell parameters of andalusite taken from Skinner et al. (1961) suggested a volumetric thermal expansion coefficient of $1.25(1) \times 10^{-2}\ ^\circ C^{-1}$, whereas those from Winter and Ghose (1979) suggested a value of $8.4(1) \times 10^{-3}\ ^\circ C^{-1}$—a difference up to about 50%. For sillimanite, the values were constrained as $6.7(3) \times 10^{-3}\ ^\circ C^{-1}$ (Skinner et al., 1961) and $4.8(1) \times 10^{-3}\ ^\circ C^{-1}$ (Winter and Ghose, 1979), so that the difference here is also close to 50%. Accordingly, more careful investigation on the thermal expansion of andalusite and sillimanite is desirable. Regarding the compressibility of the three polymorphs, the sequence of the bulk moduli is kyanite > sillimanite > andalusite, and has been better constrained than the sequence of the volumetric thermal expansion coefficients. As summarized by Liu et al. (2009), the bulk modulus of kyanite is about 196(6) GPa (when the first pressure derivative is set at 4). The values obtained by Yang et al. (1997b) for sillimanite and andalusite are 171(1) and 151(3) GPa, respectively.

Acknowledgments

We thank Professor L. Liao and one anonymous reviewer for constructive comments. This investigation was financially supported by the Natural Science Foundation of China (Grant 40872033), by the Fundamental Research Funds for the Central Universities (to XL), and by the Natural Sciences and Engineering Research Council of Canada (to MF).

References

Brace, W.F., Scholz, C.H., La Mori, P.N., 1969. Isothermal compressibility of kyanite, andalusite, and sillimanite from synthetic aggregates. Journal of Geophysical Research 74, 2089−2098.

Chatterjee, N.D., 1972. The upper stability limit of the assemblage paragonite + quartz and its natural occurrences. Contributions to Mineralogy and Petrology 34, 288−303.

Comodi, P., Zanazzi, P.F., Poli, S., Schmidt, M.W., 1997. High-pressure behavior of kyanite: compressibility and structural deformations. American Mineralogist 82, 452−459.

Friedrich, A., Kunz, M., Winkler, B., Le Bihan, T., 2004. High-pressure behavior of sillimanite and kyanite: compressibility, decomposition and indications of a new high-pressure phase. Zeitschrift Fur Kristallographie 219, 324−329.

Gatta, G.D., Nestola, F., Walter, J.M., 2006. On the thermo-elastic behaviour of kyanite: a neutron powder diffraction study up to 1200°C. Mineralogical Magazine 70, 309−317.

Hazen, R.M., Finger, L.W., 1982. Comparative Crystal Chemistry: Temperature, Pressure, Composition and the Variation of Crystal Structure. John Wiley & Sons, xv, London, 231 pp.

Irifune, T., Ringwood, A.E., Hibberson, W.O., 1994. Subduction of continental crust and terrigenous and pelagic sediments: an experimental study. Earth and Planetary Science Letters 126, 351−368.

Irifune, T., Kuroda, K., Minagawa, T., Unemoto, M., 1995. Experimental study of the decomposition of kyanite at high pressure and high temperature. In: Yukutake, T. (Ed.), The Earth's Central Part: Its Structure and Dynamics. Terra Scientific Publishing, Tokyo, pp. 35−44.

Kerrick, D.M., 1990. The Al_2SiO_5 Polymorphs. In: Reviews in Mineralogy, vol. 22. Mineralogical Society of America, Washington D.C., 406 pp.

Liu, L., 1974. Disproportionation of kyanite to corundum plus stishovite at high pressure and high temperature. Earth and Planetary Science Letters 24, 224−228.

Liu, X., Nishiyama, N., Sanehira, T., Inoue, T., Higo, Y., Sakamoto, S., 2006. Decomposition of kyanite and solubility of Al_2O_3 in stishovite at high pressure and high temperature conditions. Physics and Chemistry of Minerals 33, 711−721.

Liu, X., Shieh, S.R., Fleet, M.E., Zhang, L., 2009. Compressibility of a natural kyanite to 17.5 GPa. Progress in Natural Science 19, 1281−1286.

Matsui, M., 1996. Molecular dynamics study of the structures and moduli of crystals in the system $CaO-MgO-Al_2O_3-SiO_2$. Physics and Chemistry of Minerals 23, 345−353.

Oganov, A.R., Brodholt, J.P., 2000. High-pressure phases in the Al_2SiO_5 system and the problem of aluminous phase in the Earth's lower mantle: ab initio calculations. Physics and Chemistry of Minerals 27, 430−439.

Ono, S., Nakajima, Y., Funakoshi, K., 2007. In situ observation of the decomposition of kyanite at high pressures and high temperatures. American Mineralogist 92, 1624−1629.

Poli, S., Schmidt, M.W., 1995. H_2O transport and release in subduction zones: experimental constraints on basaltic and andesitic systems. Journal of Geophysical Research 100, 22299−22314.

Rapp, R.P., Irifune, T., Shimizu, N., Nishiyama, N., Norman, M.D., Inoue, T., 2008. Subduction recycling of continental sediments and the origin of geochemically enriched reservoirs in the deep mantle. Earth and Planetary Science Letters 271, 14−23.

Robie, R.A., Hemingway, B.S., Fisher, J.R., 1995. Thermodynamic properties of minerals and related substances at 298.15 K and 1 bar (10^5 Pascals) pressure and at high temperatures. United States Geological Survey Bulletin 2131, 461.

Schmidt, M.W., Poli, S., Comodi, P., Zanazzi, P.F., 1997. High-pressure behavior of kyanite: decomposition of kyanite into stishovite and corundum. American Mineralogist 82, 460−466.

Schmidt, M.W., Vielzeuf, D., Auzanneau, E., 2004. Melting and dissolution of subducting crust at high pressures: the key role of white mica. Earth and Planetary Science Letters 228, 65−84.

Schreyer, W., 1988. Experimental studies on metamorphism of crustal rocks under mantle pressures. Mineralogical Magazine 52, 1−26.

Skinner, B.J., Clark, S.P., Appleman, D.E., 1961. Molar volumes and thermal expansions of andalusite, kyanite, and sillimanite. American Journal of Science 259, 651−668.

Winkler, B., Hytha, M., Warren, M.C., Milman, V., Gale, J.D., Schreuer, J., 2001. Calculation of the elastic constants of the Al_2SiO_5 polymorphs andalusite, sillimanite and kyanite. Zeitschrift Fur Kristallographie 216, 67−70.

Winter, J.K., Ghose, S., 1979. Thermal expansion and high-temperature crystal chemistry of the Al_2SiO_5 polymorphs. American Mineralogist 64, 573−586.

Yang, H., Downs, R.T., Finger, L.W., Hazen, R.M., Prewitt, C.T., 1997a. Compressibility and crystal structure of kyanite, Al_2SiO_5, at high pressure. American Mineralogist 82, 467−474.

Yang, H., Hazen, R.M., Finger, L.W., Prewitt, C.T., Downs, R.T., 1997b. Compressibility and crystal structure of sillimanite, Al_2SiO_5, at high pressure. Physics and Chemistry of Minerals 25, 39−47.